Analysis of the Generalized Order Statistics Constant False Alarm Rate Detector

Chang-Joo Kim and Hwang-Soo Lee

CONTENTS

ABSTRACT

In this paper, we present an architecture of the *constant false alarm rate* (CFAR) detector called the *generalized order statistics* (GOS) CFAR detector, which covers various *order statistics* (OS) and *cell-averaging* (CA) CFAR detectors as special cases. For the proposed GOS CFAR detector, we obtain unified formulas for the false alarm and detection probabilities. By properly choosing coefficients of the GOS CFAR detector, one can utilize any combination of ordered samples to estimate the background noise level. Thus, if we use a reference window of size N, we can realize $(2^N - 1)$ kinds of CFAR processors and obtain their performances from the unified formulas. Some examples are the CA, the OS, the *censored mean level*, and the *trimmed mean* CFAR detectors. As an application of the GOS CFAR detector to multiple target detection, we propose an algorithm called the *adaptive mean level detector*, which censors adaptively the interfering target returns in a reference window.

I. INTRODUCTION

The *constant false alarm rate* (CFAR) detection is a signal processing technique to control false alarm rate for automatic target detection in radar systems. Since the background clutter-plus-noise level is unknown and time-varying at any given location, the radar detector with a fixed threshold can not be applied to the radar returns if one wants to control the false alarm rate. The CFAR detection technique is employed to control the false alarm rate, which estimates the background clutter-plus-noise level and sets a threshold adaptively based on the local information of clutter-plus-noise level.

In the conventional *cell-averaging* (CA) CFAR detector [1], the background level is estimated by averaging the outputs of the neighboring resolution cells (range and/or Doppler) under the assumption that the background level is homogeneous. As the number of cells utilized in estimating the mean level increases, the probability of detection approaches that of the classical Neyman-Pearson case where the mean level of clutter-plus-noise is known *a priori*, provided that these cells do not contain interfering target returns. However, most CFAR processors cannot maintain the optimal performance when homogeneous assumption is violated.

There are two cases of nonhomogeneous situations. One is the step change in background level, which may be observed at clutter edge. If the test cell is in the clear region but a group of the reference cells are in the clutter region, a masking effect results. On the other hand, if the test cell is in the clutter region but some of the reference cells are in the clear region, then false alarm increases with an increase in the clutter level discontinuity.

The other case of nonhomogeneous situations results from interfering target returns. Interfering targets present in the reference window, which have different statistics from the background statistics, raise the threshold and result in reduced detection probability. The more range (and/or Doppler) cells that are used in calculating the threshold, the greater the likelihood of encountering interfering target returns. There exists a trade-off between maintaining homogeneity and reducing the loss in signal-to-noise ratio (SNR) by increasing the number of window cells. Rickard and Dillard [2] have proposed to censor a few of the largest reference cells and use only the remaining cells to estimate the background clutter-plus-noise level. The *censored mean level detector* (CMLD) exhibits a small additional CFAR loss in a homogeneous noise situation and is quite robust in the presence of interfering targets as long as the number of cells censored exceeds the number of interferers.

In the *order statistics* (OS) CFAR detector, proposed by Rohling [3], the input data in a reference window are sorted in an increasing order. The threshold is scalar times a single quantile, the k-th smallest cell in the reference

window. This concept provides inherent protection against a drastic drop in performance in the presence of interfering targets. However, there is some CFAR loss of detection probability in the OS CFAR detector compared with that of the CA CFAR detector in homogeneous situation.

On the other hand, the *trimmed mean* (TM) CFAR detector with proper choice of the trimming parameters, introduced by Gandhi and Kassam [4], can be a compromise between the CA CFAR and the OS CFAR processors. The TM CFAR processor first orders the reference cells according to their magnitudes and then trims T_1 cells from the lower end and T_2 cells from the upper end. Finally the background level is estimated by summing the remaining cells after censoring.

In this paper, we introduce the *generalized order statistics* (GOS) CFAR detector, which includes the OS CFAR, the CA CFAR, the CMLD, and the TM CFAR detectors as special cases. As an application of the GOS CFAR detector to multiple target detection, we also introduce the *adaptive mean level detector* (AMLD).

This paper is organized as follows. Following this Introduction, the GOS CFAR detector is introduced and analyzed in Section II. In Section III, we obtain and discuss its analytical results. In Section IV, we propose a new adaptive censoring scheme and obtain its performance. Finally, Conclusions are made in Section V.

II. GOS CFAR DETECTOR

The GOS CFAR processor first orders samples of range cells according to their magnitudes. Then it multiplies the ordered samples by the corresponding coefficients of the GOS filter and sums the results to form an estimate of the clutter-plus-noise level as shown in Fig. 1. The output Z of the GOS filter of window size N is obtained as

$$Z = \sum_{i=1}^{N} \alpha_i X_{(i)} \tag{1}$$

where $X_{(i)}$ is the i-th smallest sample among N samples in the reference window, and $\{\alpha_i\}_{i=1}^{N}$ is a set of binary weights that can be chosen properly for a specific application. Then, this estimate is multiplied by a threshold coefficient T to yield the adaptive threshold against which the output of the cell under test will be compared. There may be $(2^N\text{-}1)$ kinds of CFAR processors obtained by combinations of $\{\alpha_i\}_{i=1}^{N}$ in the GOS CFAR detector. By proper choice of the coefficients of the GOS filter, the GOS CFAR detector becomes the CA CFAR detector, which is a linear CFAR processor, or the nonlinear CFAR processor, such as the OS CFAR detector.

To show the relationship between the GOS CFAR detector and other CFAR processors, we denote the GOS CFAR detector as GOS$(n_1, n_2, \ldots, n_i, \ldots)$ CFAR processor, where n_i represents the position of each coefficient of the GOS filter whose value is 1. For example, the OS(k) CFAR detector can be

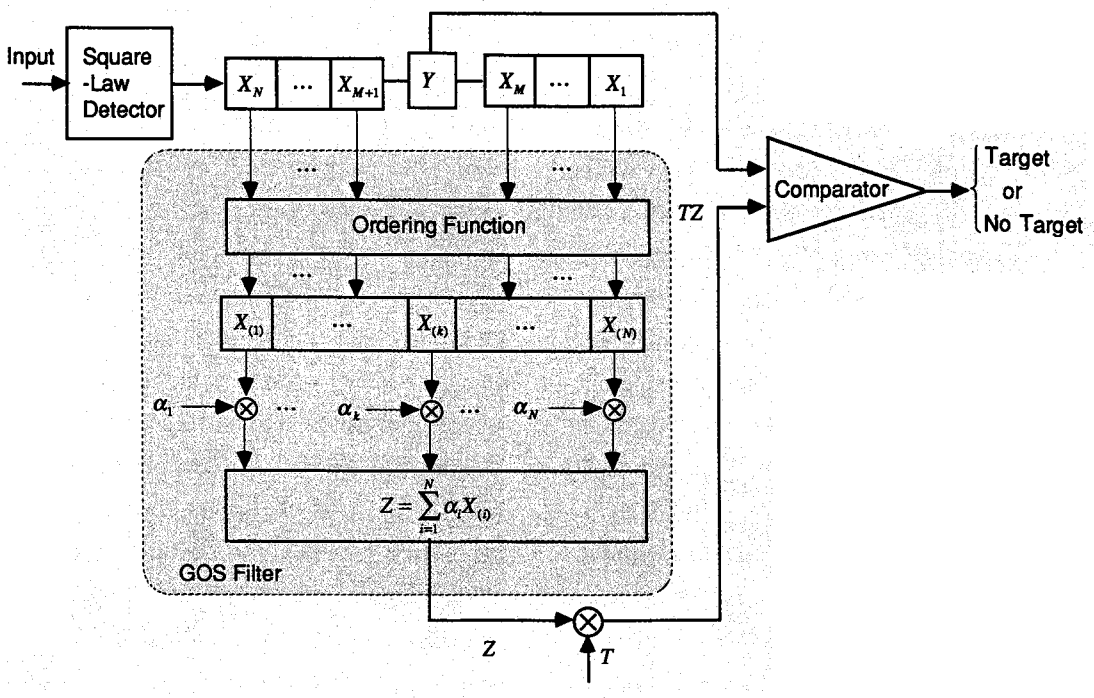

Fig. 1. Structure of the GOS CFAR detector.

represented as the GOS(k) CFAR processor, and the CA CFAR detector as the GOS $(1, 2, \ldots, N)$ CFAR processor, and the TM CFAR detector as the GOS($T_1+1, \ldots, N-T_2$) CFAR processor, and CMLD as the GOS $(1, \ldots, N-T_2)$ CFAR processor. In this way, we can implement the GOS CFAR detectors ranging from GOS(1) to GOS$(1, 2, \ldots, N)$ CFAR processors. The GOS( ) CFAR processor does not exist because it means Z=0.

To obtain detection performance of an adaptive threshold detector, we need the probability density function (pdf) of the CFAR threshold, which is a random variable depending on the statistics of clutter-plus-noise. Then, given a desired false alarm rate, we can evaluate the detection probability from the moment generating function (mgf) of the adaptive threshold.

We assume that the square-law detected output for any range cell is exponentially distributed (Swerling I statistics), with pdf

$$p(x) = \frac{1}{2\sigma^2\rho} \exp\left(-\frac{x}{2\sigma^2\rho}\right) \qquad (2)$$

where

$$\rho = \begin{cases} 1, & \text{under } H_0 \\ (1+S), & \text{under } H_1 \end{cases}$$

and S is SNR of a target, and σ^2 is thermal noise power.

A target is declared to be present if the magnitude of the test cell, Y, exceeds the threshold TZ. Here T is a threshold coefficient to achieve a desired false alarm probability for a given window size N and Z is the estimate of background clutter-plus-noise level. The performance of a CFAR processor is represented by the average detection and the false alarm probabilities depending upon the random variable Z. The false alarm probability is determined by

$$\begin{aligned} P_{fa} &= E_Z\left\{P[Y > TZ|H_0]\right\} \\ &= E_Z\left[\int_{TZ}^{\infty} \frac{1}{2\sigma^2}\exp\left(-\frac{x}{2\sigma^2}\right)dx\right] \\ &= E_Z\left[\exp\left(-\frac{TZ}{2\sigma^2}\right)\right] \\ &= M_Z\left[\frac{T}{2\sigma^2}\right] \end{aligned} \tag{3}$$

where $M_Z[\cdot]$ is mgf of the random variable Z.

The detection probability is obtained by

$$\begin{aligned} P_d &= E_Z\left\{P[Y > TZ|H_1]\right\} \\ &= E_Z\left[\int_{TZ}^{\infty} \frac{1}{2\sigma^2(1+S)} \right. \\ &\quad \left. \times \exp\left(-\frac{x}{2\sigma^2(1+S)}\right)dx\right] \\ &= E_Z\left[\exp\left(-\frac{TZ}{2\sigma^2(1+S)}\right)\right] \\ &= M_Z\left[\frac{T}{2\sigma^2(1+S)}\right]. \end{aligned} \tag{4}$$

1. Analysis of the GOS CFAR Processor in Homogeneous Situation

The test statistic of the GOS CFAR processor is given by (1). Even if the original samples $\{X_1, X_2, \ldots, X_N\}$ are independent and identically distributed (i.i.d.) random variables, the ordered statistics $\{X_{(1)}, X_{(2)}, \ldots, X_{(N)}\}$ are not i.i.d. However, assuming that $\{X_1, X_2, \ldots, X_N\}$ are exponentially distributed, the following transformation to random variables $\{W_1, W_2, \ldots, W_N\}$ results in independent quantities [4,5]:

$$W_i = X_{(i)} - X_{(i-1)} \tag{5}$$

where $X_{(0)} = 0$. To get pdf of W_i, we use the joint pdf of $X_{(r)}$ and $X_{(s)}$, $1 \le r \le s \le N$. The joint pdf of $X_{(r)}$ and $X_{(s)}$ is given by [5]

$$\begin{aligned} f_{rs}(x, y) = &\frac{N!}{(r-1)!(s-r-1)!(N-s)!} \\ &\times [P(x)]^{r-1} p(x) \\ &\times [P(y) - P(x)]^{s-r-1} \\ &\times p(y)[1 - P(y)]^{N-s}, x \le y \end{aligned} \tag{6}$$

where

$$p(x) = \frac{1}{2\sigma^2}\exp\left(-\frac{x}{2\sigma^2}\right),$$

$$p(y) = \frac{1}{2\sigma^2}\exp\left(-\frac{x}{2\sigma^2}\right),$$

$$P(x)=1-\exp\left(-\frac{x}{2\sigma^2}\right),$$

and $$P(y)=1-\exp\left(-\frac{y}{2\sigma^2}\right).$$

By taking $s=i$ and $r=i-1$, and then replacing y with $x+W_i$, we obtain

$$\begin{aligned} f_{rs}(x,x+W_i) &= \frac{N!}{(i-2)!(N-i)!} \\ &\times\left[1-\exp\left(-\frac{x}{2\sigma^2}\right)\right]^{i-2} \\ &\times\frac{1}{2\sigma^2}\exp\left(-\frac{x}{2\sigma^2}\right) \\ &\times\frac{1}{2\sigma^2}\exp\left(-\frac{x+W_i}{2\sigma^2}\right) \\ &\times\left[1-\exp\left(-\frac{x+W_i}{2\sigma^2}\right)\right]^{N-i} \end{aligned} \quad (7)$$

After integrating (7) with respect to x, we have

$$\begin{aligned} f_{rs}(W_i) &= \int_0^\infty f_{rs}(x,x+W_i)dx \\ &= \int_0^\infty \frac{N!}{(i-2)!(N-i)!} \\ &\times\left[1-\exp\left(-\frac{x}{2\sigma^2}\right)\right]^{i-2} \\ &\times\frac{1}{2\sigma^2}\exp\left(-\frac{x}{2\sigma^2}\right) \\ &\times\frac{1}{2\sigma^2}\exp\left(-\frac{x+W_i}{2\sigma^2}\right) \\ &\times\left[1-\exp\left(-\frac{x+W_i}{2\sigma^2}\right)\right]^{N-i} dx \\ &= \frac{1}{2\sigma^2}(N-i+1) \\ &\times\exp\left(-\frac{(N-i+1)W_i}{2\sigma^2}\right). \end{aligned} \quad (8)$$

Now, let us consider the following transformation:

$$V_i=\sum_{j=i}^{N}\alpha_j W_i. \quad (9)$$

The estimate Z is given by

$$Z=\sum_{i=1}^{N}V_i. \quad (10)$$

We can obtain mgf of Z from the product of the individual mgf of $V_i's$ because the random variables $W_i's$ are independent.

$$\begin{aligned} M_{V_i}(T) &= E\left[\exp(-TV_i)\right] \\ &= E\left[\exp\left(-T\sum_{j=i}^{N}\alpha_j W_i\right)\right] \\ &= \frac{N-i+1}{(N-i+1)+2\sigma^2 T\sum_{j=i}^{N}\alpha_j}. \end{aligned} \quad (11)$$

The false alarm probability is found to be

$$\begin{aligned} P_{fa} &= \prod_{i=1}^{N} M_{V_i}\left(\frac{T}{2\sigma^2}\right) \\ &= \prod_{i=1}^{N}\frac{N-i+1}{N-i+1+T\sum_{j=i}^{N}\alpha_j}. \end{aligned} \quad (12)$$

As a special case, let us consider that the coefficients of the GOS filter are given by

$$\alpha_j=\begin{cases}1, & j=k\\ 0, & j\neq k\end{cases} \quad 1\le k\le N. \quad (13)$$

In this case,

$$\sum_{j=i}^{N}\alpha_j=\begin{cases}1, & i\le k\\ 0, & i>k.\end{cases} \tag{14}$$

Thus (12) becomes

$$\begin{aligned}P_{fa}&=\prod_{i=1}^{N}\frac{N-i+1}{N-i+1+T\sum_{j=i}^{N}\alpha_j}\\&=\frac{N}{N+T}\,\frac{N-1}{N-1+T}\times\cdots\\&\quad\times\frac{N-(k-1)+1}{N-(k-1)+1+T}\,\frac{N-k+1}{N-k+1+T}\\&\quad\times\frac{N-k}{N-k}\times\cdots\times\frac{1}{1}\\&=k\binom{N}{k}\frac{(k-1)!\,(N+T-k)!}{(N+T)!}.\end{aligned} \tag{15}$$

This corresponds to the equation of false alarm probability for the OS CFAR processor obtained by Rohling [3]. Also, if we set all the coefficients of the GOS filter to one, then

$$\sum_{j=i}^{N}\alpha_j=N-i+1. \tag{16}$$

Therefore, the false alarm probability becomes

$$P_{fa}=[1+T]^{-N}. \tag{17}$$

This represents the false alarm probability for the CA CFAR processor. From the above results, we can see that the general expression for the performance of the GOS CFAR processor includes that of the OS CFAR processor as well as that of the CA CFAR processor as a special case in homogeneous situation.

Finally, the detection probability can be obtained as

$$\begin{aligned}P_d&=\prod_{i=1}^{N}M_{V_i}\left(\frac{T}{2\sigma^2(1+S)}\right)\\&=\prod_{i=1}^{N}\frac{N-i+1}{N-i+1+\dfrac{T}{1+S}\sum_{j=i}^{N}\alpha_j}.\end{aligned} \tag{18}$$

2. Analysis of the GOS CFAR Processor in Nonhomogeneous Situation

In order to obtain the general formula for the performance of the GOS CFAR processor in nonhomogeneous environments, we follow the approach of Blake [6], in which all the background cells have Swerling I statistics with the clutter-to-thermal noise ratio (CNR) in the i-th cell denoted by C_i. If the j-th cell contains only thermal noise, then $C_j=0$.

The transformation from $\{X_1,\ldots,X_N\}$ to $\{X_{(1)},\ldots,X_{(N)}\}$ is not one-to-one. There is a total of $N!$ possible arrangements of $\{x_{(1)},\ldots,x_{(N)}\}$ in increasing order of magnitude. Thus, there are $N!$ inverses to the transformation.

The mgf of the clutter-plus-noise estimator is obtained as

$$\begin{aligned}M_Z(s)&=E_Z\left[\exp(-sZ)\right]\\&=E_Z\left[\exp\left(-s\sum_{i=1}^{N}\alpha_i X_{(i)}\right)\right]\\&=\sum_{\text{all N! inverses}}\int_0^{\infty}dx_{(1)}\frac{\exp\left(-\dfrac{x_{(1)}}{2\sigma^2\beta_{(1)}}\right)}{2\sigma^2\beta_{(1)}}\end{aligned}$$

$$\times\cdots\times\int_{x_{(N-1)}}^{\infty} dx_{(N)}\frac{\exp\left(-\frac{x_{(N)}}{2\sigma^2\beta_{(N)}}\right)}{2\sigma^2\beta_{(N)}}$$

$$\times\exp\left(-s\sum_{i=1}^{N}\alpha_i x_{(i)}\right)$$

$$=\sum_{\text{all N! inverses}}\prod_{i=1}^{N}\frac{1}{2\sigma^2\beta_{(i)}}$$

$$\times\left(\sum_{j=i}^{N}\left(\frac{1}{2\sigma^2\beta_{(i)}}+s\alpha_j\right)\right)^{-1} \quad (19)$$

where $\beta_{(i)}=1+C_{(i)}$ and $C_{(i)}$ is CNR of background cell ranked in the i-th place after ordering the background cells in the reference window.

Therefore, the false alarm probability is given by

$$P_{fa}=M_Z\left(\frac{T}{2\sigma^2}\right)$$

$$=\sum_{\text{all N! inverses}}\prod_{i=1}^{N}\frac{1}{\beta_{(i)}}$$

$$\times\left(\sum_{j=i}^{N}\left(\beta_{(j)}^{-1}+T\alpha_j\right)\right)^{-1}. \quad (20)$$

With $C_{(i)}=0$, (20) becomes (12), i.e.,

$$P_{fa}=N!\prod_{i=1}^{N}\left(\sum_{j=i}^{N}(1+T\alpha_j)\right)^{-1}$$

$$=\prod_{i=1}^{N}\frac{N-i+1}{N-i+1+T\sum_{j=i}^{N}\alpha_j}. \quad (21)$$

On the other hand, the detection probability is given by

$$P_d=\sum_{\text{all N! inverses}}\prod_{i=1}^{N}\frac{1}{\beta_{(i)}}$$

$$\times\left(\sum_{j=i}^{N}\left(\frac{1}{\beta_{(j)}}+\frac{T\alpha_j}{1+S}\right)\right)^{-1} \quad (22)$$

III. ANALYTICAL RESULTS AND DISCUSSION

Using the unified formulas proposed for the performance of the CFAR processors, we first obtain the detection performance of the various CFAR detectors in homogeneous and multiple target situations. Next, we analyze the false alarm rates for several CFAR processors at clutter edge. In this analytical study, we set the reference window size (N) to 24, the desired false alarm rate (FAR) P_{fa} to 10^{-6}, and interfering target signal to noise ratio(INR) to 30 dB.

Fig. 2 shows the detection performance of the CA CFAR, the OS CFAR, and the GOS(1,...,21) CFAR processor in homogeneous situation. As we might expect, the CA CFAR detector has the best detection performance. Also shown is that the GOS (1,...,21) CFAR detector yields better detection performance than the OS(21) CFAR detector. The background level of the GOS(1,...,21) is estimated by $Z=X_{(1)}+\ldots+X_{(21)}$.

In Fig. 3, the detection probability is plotted as a function of SNR of the primary target

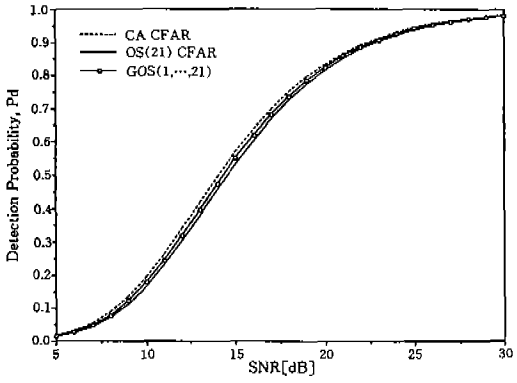

Fig. 2. Detection probabilities vs. target SNR in homogeneous situation.

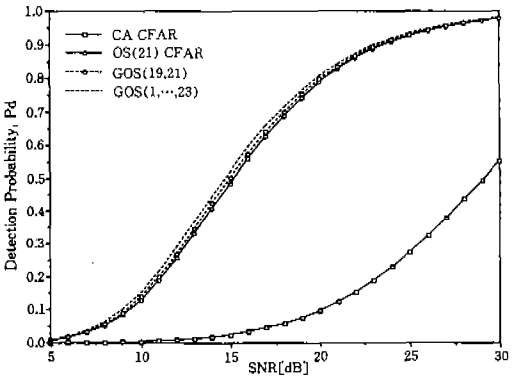

Fig. 3. Detection probabilities vs. target SNR with one interfering target (INR=30 dB).

with INR = 30 dB when there exists one interfering target in a reference window. From this figure, we can see that even though there exists only one interfering target in a reference window, the detection performance of the CA CFAR processor is seriously degraded. However, the OS(21), the GOS(1,...,23), and

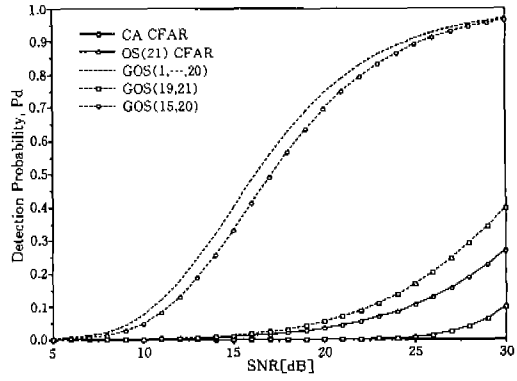

Fig. 4. Detection probabilities vs. target SNR with four interfering targets (INR=30 dB).

the GOS(19,21) CFAR processors reveal little degradation from an interfering target. Here the background level of the GOS(1,...,23) CFAR processor is estimated by $Z = X_{(1)} + \ldots + X_{(23)}$ and the GOS(19,21) by $Z = X_{(19)} + X_{(21)}$. The detection performance of the GOS(1,...,23) CFAR processor has the best performance in this situation.

Fig. 4 shows the detection performance when there exist four interfering target returns in the reference window. In this case, the detection performances of the GOS(1,...,20) and the GOS(15,20) CFAR detectors are good, while those of both the OS(21), the GOS(19,21), and the CA CFAR processors are severely degraded. This is the reason that the GOS (1,...,20) and GOS(15,20) CFAR detectors can handle up to four interfering target returns while the OS(21) CFAR and GOS(19,21) CFAR processors can handle only three

interfering targets. If there exist five interfering targets in the reference window, the detection performance of the GOS(15,20) CFAR detector shall be seriously degraded.

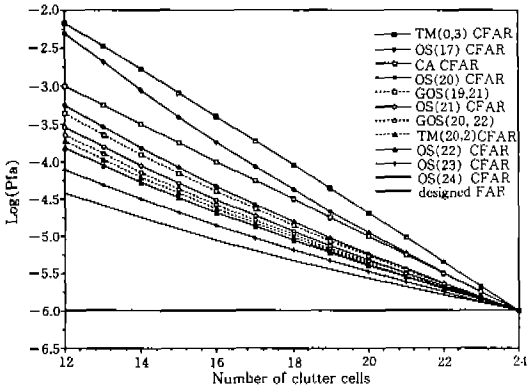

Fig. 5. False alarm rates at clutter edge (CNR=30 dB).

In order to obtain the performance of each CFAR processor at clutter edge, we compare the false alarm rate as a function of the number of the clutter cells as shown in Fig. 5. In this figure, we assume that the test sample is from the clutter region and CNR=30 dB. Here the background level of the GOS(20,22) CFAR processor is estimated by $Z = X_{(20)} + X_{(22)}$. From the figure, one can notice that the false alarm rates of both the GOS(20,22) CFAR processor and the TM(20,2) CFAR processor are between those of the OS(21) CFAR processor and the OS(22) CFAR processor. And the false alarm rates of the the GOS(19,21) CFAR processor are worse than that of the OS(21) CFAR processor. Therefore, we notice that as long as T_2 is fixed, the larger T_1, the better performance in false alarm rate because the background estimator uses less of small clutter-plus-noise samples. The TM(23,0) CFAR detector, which is equivalent to the OS(24) CFAR processor, has the lowest performance sensitivity for the false alarm rate, but the capturing effect, which is occurred by raising the threshold due to the uncensored interference in multiple target situations, is most severe. Also, one should notice that the performance of the OS(17) CFAR processor and the TM(0,3) CFAR processor are worse than that of the CA CFAR detector. When we compare the performance between the GOS(19,21) CFAR detector and the OS(21) CFAR detector, the GOS(19,21) reveals better performance in multiple target situations while the OS(21) CFAR detector does at clutter edge. In this situation, the false alarm rate is controlled if the background level is estimated only with the clutter samples from the clutter region after censoring the noise samples from the clear region. This ideal performance can be obtained by adaptive scheme that estimates exactly the number of noise samples from the clear region.

IV. APPLICATION OF THE GOS CFAR DETECTOR TO MULTIPLE TARGET DETECTION

Since target capturing is experienced un der multiple target situation, it is necessary to reduce the capturing effect to a minimum. If

interfering targets of strong magnitude appear in the reference window, they occupy the highest positions in the ordered cells with high probability. So, we can avoid the capturing effects due to interfering targets by ordering the background noise samples to their magnitudes and discarding properly those from the interfering target returns.

The CMLD needs *a priori* information of the number of interfering target returns in multiple target situation. So, target capturing may occur. An adaptive scheme is required to estimate the number of interferers. Approaches, such as the Barboy's multistep procedure [7] and the Barkat's method [8], censor adaptively the interfering target returns in the reference window. However, the simulation result by Barkat [8] shows that the Barboy's multistep procedure cannot maintain the robustness when the number of cells are small. On the other hand, to operate the CFAR detector in real time, the computational complexity is an important factor. In this paper, we also introduce the *adaptive mean level detector* (AMLD), which has better detection performance than the *generalized censored mean level detector* (GCMLD), and also reduce efficiently the computational complexity when there exist a few interfering targets in the reference window.

In this section, we introduce the AMLD algorithm for censoring the interfering target returns and obtain its performance.

1. AMLD

To exclude interfering target returns in a reference window, we should utilize all the status information of each background cell in the reference window. We divide the reference window into a leading window and a lagging window. The status information of each cell in the lagging window can be easily obtained by comparing the cell under test with the estimated threshold ($TZ/2$). However, the status information of each cell in the leading window cannot be obtained from the conventional CFAR structures.

In AMLD, we modify the conventional CFAR structure to obtain the status information of each cell in the leading window. Different from the other CFAR processors, AMLD has two test cells. Beside a test cell at the center of a window as that used in the conventional CFAR detectors, AMLD use one more cell called the pre-test cell, which will be entered into the reference window at the next time. Let the content of the pre-test cell be Y_o.

The block diagram of AMLD is shown in Fig. 6. To illustrate the AMLD algorithm more clearly, a timing diagram of the data flow in AMLD is shown in Fig. 7 when the window size is 4. We assume that there are 10 input data cells denoted by 1 to 10 in a sequential order. At each time instant, all the cells in the window shift right one place to exclude the oldest cell and obtain new one.

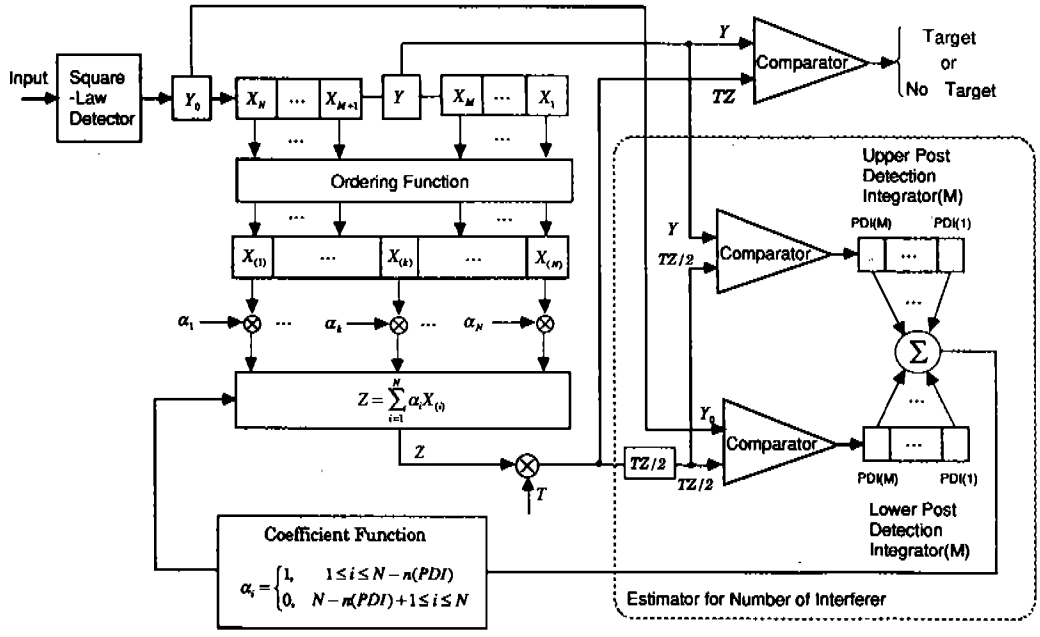

Fig. 6. Structure of AMLD.

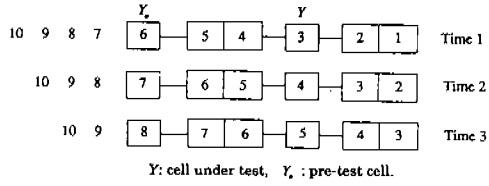

Fig. 7. Timing diagram of the data flow in AMLD.

In order to remove the interfering target returns in AMLD, the pre-test cell Y_o and the cell under test Y are compared with the threshold level and the results of each test stored in the lower and upper *post detection integrator* (PDI) registers, respectively. If Y_o exceeds $(TZ/2)$, then 1 is stored in the lower PDI shift register in Fig. 6. Otherwise, 0 is stored. Also, if Y exceeds $(TZ/2)$, then 1 is stored in the upper PDI shift register. Otherwise, 0 is stored. The PDI registers can be set by both false alarms and target returns, but the false alarms are negligible. The number of interferers can be estimated by simply summing the number of 1's in the PDI registers. Fig. 8 shows the overall operation of AMLD.

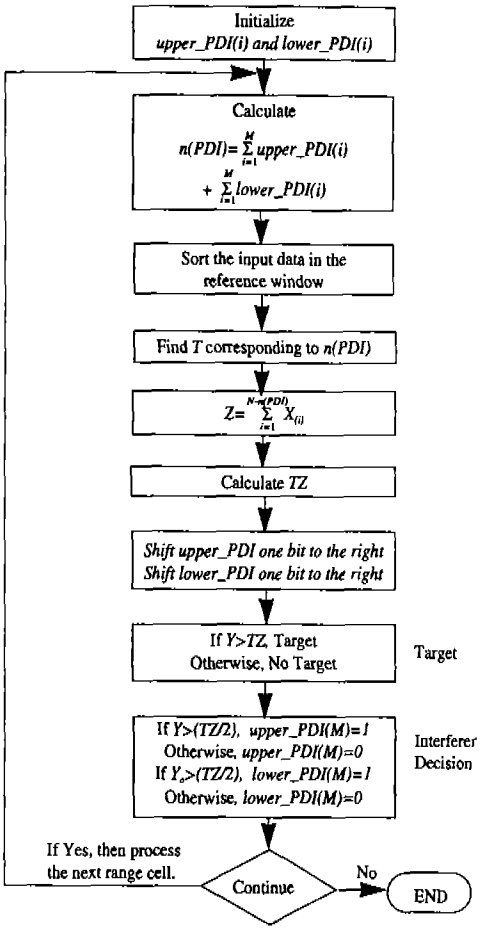

Fig. 8. Flowchart for operation of AMLD.

2. Probabilities of Detection and False Alarm

In multiple target situations, let us suppose that the reference window contains $n(PDI)$ interfering target returns with the power level of $(1+I)/2$ and $N-n(PDI)$ noise cells with power level of (1/2) where I denotes the average INR. Also, let us assume that INRs of all the interfering target returns are the same. Given the estimated $n(PDI)$ and INRs of the interfering targets, the detection and false alarm probabilities are obtained as

$$P_d = \sum_{n(PDI)=0}^{N-1} P_{d|n(PDI)} Pr\left[n(PDI)\right] \quad (23)$$

$$P_{fa} = \sum_{n(PDI)=0}^{N-1} P_{fa|n(PDI)} Pr\left[n(PDI)\right] \quad (24)$$

and

$$P_{d|n(PDI)} = \sum_{\text{all N! inverses}} \prod_{i=1}^{N} \frac{1}{1+I_{(i)}} \times \left(\sum_{j=i}^{N} \left(\frac{1}{1+I_{(j)}} + \frac{T\alpha_j}{1+S} \right) \right)^{-1} \quad (25)$$

$$P_{fa|n(PDI)} = \sum_{\text{all N! inverses}} \prod_{i=1}^{N} \frac{1}{1+I_{(i)}} \times \left(\sum_{j=i}^{N} \left(\frac{1}{1+I_{(j)}} + T\alpha_j \right) \right)^{-1} \quad (26)$$

where $I_{(i)}$ is I or 0 depending on the existence of an interferer or not.

We can obtain the probabilities of false alarm and detection in multiple target situation by setting the coefficients of the GOS filter as

$$\alpha_i = \begin{cases} 1, & 1 \le i \le N - n(PDI) \\ 0, & \text{otherwise.} \end{cases} \quad (27)$$

Table 1. Computational complexities of GCMLD and AMLD ($N=2M$).

NO. of Interferers	GCMLD				AMLD			
	Add	Multiply	Compare	Sort	Add	Multiply	Compare	Sort
0	$2(M-2)+1$	$2(M-1)$	$2(M-1)$	$2O(M\log_2 M)$	4	1	2	$O(N\log_2 N)$
1	$(2M-5)+1$	$2M-3$	$2M-3$	$2O(M\log_2 M)$	4	1	2	$O(N\log_2 N)$
2	$2(M-3)+1$	$2M-4$	$2M-4$	$2O(M\log_2 M)$	4	1	2	$O(N\log_2 N)$

3. Computational Complexity of AMLD

We obtain the computational complexity of the proposed AMLD algorithm in estimating the number of interferers and compare the result with that of the GCMLD introduced by Barkat [6]. The estimator to obtain the number of interfering targets in AMLD consists of two shift registers with size M, an adder, a divider, and two comparators to test the pre-test cell in addition to the original comparator. Table 1 shows the computational complexities for a few interfering target returns. In this Table, subtract operations in AMLD are included in add operations and the number of add operations at the initial time is N in AMLD. If there are two interfering targets in the reference window with size $N=24$, the number of computations for each operation is obtained as follows:

GCMLD : *Add=19, Multiply=20, Compare=20, and Sort= 96*

AMLD : *Add= 4, Multiply= 1, Compare= 2, and Sort=120.*

Since AMLD uses the reference window as a whole while GCMLD divides that into the leading and lagging windows in sorting, the computational complexity of sorting in AMLD is greater than that of GCMLD. However, computational complexities in terms of add, multiply, and compare operations of AMLD are far less than those of GCMLD.

On the other hand, GCMLD has a merit to obtain the background level estimate, Z, in this censoring process while AMLD needs $N-n(PDI)$ extra summations to get it. However, GCMLD needs an additional procedure (e.g. reading a look-up table) to obtain threshold coefficient T_i per each iteration in the cen-

soring process, while AMLD does not need such threshold coefficients except the final T.

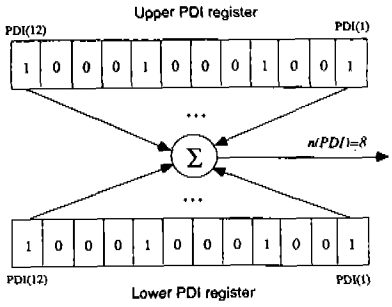

Fig. 9. Initial data of PDI registers used in simulation.

4. Simulation Example of the AMLD Operation

The initial condition of AMLD is important, but simple. As long as the initial value, i.e., $n(PDI)$, is greater than or equal to the number of interfering targets in the reference window, AMLD operates steadily. Therefore, it is recommended that $n(PDI)$ at the initial time should be set to a larger value. In this section, we show one example of the AMLD operation. The level of background noise power is 20 dB and INR is 20 dB. The size of the reference window is 24. Between range cell 20 and range cell 60, there exist $2 \sim 6$ targets in the reference window. In this simulation, we select $n(PDI) = 8$ at the initial time as shown in Fig. 9.

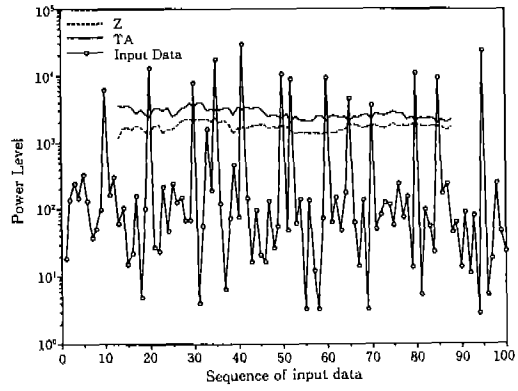

Fig. 10. Behavior of AMLD in multiple target situations (INR=20 dB).

Fig. 10 shows the relationships between the input data used in this simulation, the threshold (TZ), and the estimate of background level (Z). From the figure, we can see that the AMLD detects all the targets except range cell 33. Since the target signal fluctuates with Swerling I model, target may be missed like at a range cell 33. However, AMLD performs well without the effects of the interfering targets because the estimator for the number of interfering target can detect all the targets in this simulation as shown in Fig. 11. Fig. 11 shows the relationship between the number of interfering targets in the reference window and its estimate obtained by AMLD. From the figure, one can notice that just after M time instances from the initial time operation, the number of interfering targets estimated by AMLD is the same as that of actual interfering targets in the reference window. M is the the maximum time

duration that the number of interfering targets estimated by AMLD converges to the number of actual interfering targets in the reference window from the initial time. Simulation results show that AMLD also performs well even though the number of interfering targets changes with time.

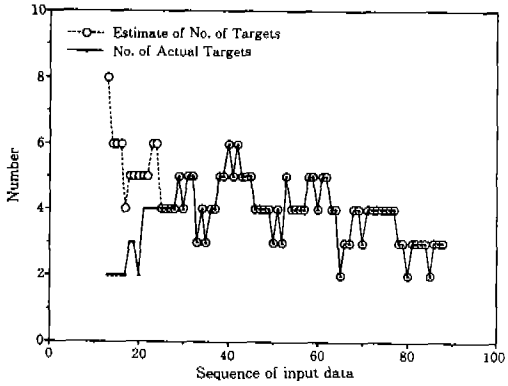

Fig. 11. Relationship between the number of interfering targets and its estimate in AMLD (INR=20 dB).

5. Simulation Results and Discussion

In this section, we compare the performance of AMLD with that of GCMLD. Since the $\Pr[n(PDI)]$ is difficult to obtain mathematically, the performance of AMLD is evaluated by computer simulations. The results are obtained after 100,000 trial simulation. In this simulation study, we set the reference window size (N) to 24, the designed FAR to 10^{-6}, and the designed probability of the false censoring (P_{FC}) is equal to the designed FAR. All the probabilistic data used in this simulation are obtained by the IMSL statistical library.

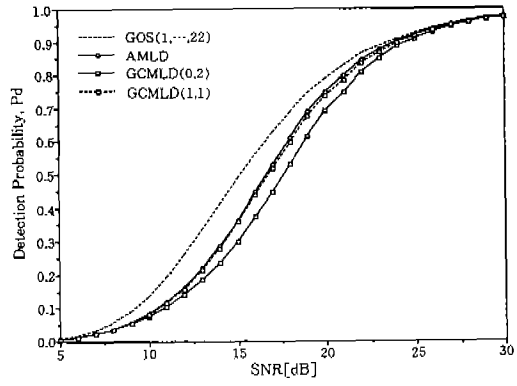

Fig. 12. Simulated detection probability of AMLD and GCMLD for two interfering targets (I/S=1).

Fig. 12 shows the detection performance of AMLD and GCMLD when there exist two interfering targets in the reference window. GCMLD(0,2) in this figure means that two interfering targets are present in leading window or lagging window. GCMLD(1,1) means that there exists one interfering target in leading and lagging window, respectively. The GOS(1, ..., 22) CFAR detector has the maximum detection performance in this situation. We can see that AMLD has slightly better detection performance than GCMLD(1,1). Also shown is that the performance of GCMLD(0,2) is worse than that of GCMLD(1,1).

Fig. 13 shows the detection performance of AMLD and GCMLD when there exist four interfering targets in a reference window. The GOS(1, ..., 20) CFAR detector yields the maximum detection performance in this situa-

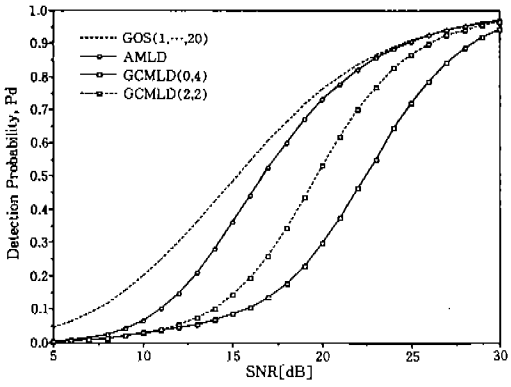

Fig. 13. Simulated detection probability of AMLD and GCMLD for four interfering targets (I/S=1).

tion. We can see that AMLD has better detection performance than GCMLD. Also shown is that the performance of GCMLD(0,4) is worse than that of GCMLD(2,2).

V. CONCLUSIONS

In this paper, we propose the GOS CFAR processor, a generalized structure of the OS CFAR processors. And a unified formula for the false alarm probability in homogeneous as well as nonhomogeneous situations is derived in a closed form. By properly choosing the coefficients of the GOS filter, we can obtain the OS CFAR processor, the TM CFAR processor, and the CMLD as well as the CA CFAR processor as special cases. Using the unified CFAR structure and the performance formula, we compare the detection performance of various CFAR processors in homogeneous and multiple target situations and false alarm performance at clutter edge. In homogeneous situation, the CA CFAR detector, which is equivalent to the GOS$(1, \ldots, N)$ CFAR detector, has the best detection performance, but it exhibits serious performance degradation in nonhomogeneous situations. When there exist the interfering targets in the reference window, it is desired to design the CFAR detector that estimates, the background level with all the remaining samples after censoring the interference samples. On the other hand, from an analysis of the false alarm performance at clutter edge, we can see that to control the false alarm, it is desirable to estimate the background level with the ordered samples at high position after removing the noise samples from the clear region.

As an application of the GOS CFAR detector to multiple target situation, we compared the detection performance of AMLD and GCMLD. The simulation results show that the former can have better detection performance than the latter. AMLD also has less computational complexity than GCMLD. As an another application, we are now studying the modified AMLD algorithm to regulate the false alarm rate at clutter edge.

REFERENCES

[1] H. M. Finn and R. S. Johnson, "Adaptive detection mode with threshold control as a function of spatially sampled clutter level estimates," *RCA review*, vol.29, no.3, Sept. 1968, pp.414-464.

[2] J. T. Rickard and G. M. Dillard, "Adaptive Detection Algorithms for Multiple Target Situations," *IEEE Transactions on Aerospace and Electronics Systems,* AES-13, no.4, July 1977, pp.338-343.

[3] H. Rohling, "Radar CFAR Thresholding in Clutter and Multiple Target Situations," *IEEE Transactions on Aerospace and Electronics Systems,* AES-19, no.4, July 1983, pp.608-621.

[4] P. P. Gandhi and S. A. Kassam, "Analysis of CFAR Processors in Nonhomogeneous Background," *IEEE Transactions on Aerospace and Electronics Systems,* AES-24, no.4, July 1988, pp.427-445.

[5] H. A. David, *Order Statistics*, New York: Wiley,1981.

[6] S. Blake, "OS CFAR Theory for Multiple Targets and Nonuniform Clutter," *IEEE Transactions on Aerospace and Electronics Systems,* AES-24, no.4, Nov. 1988, pp.785-790.

[7] B. Barboy A. Lomes and E. Perkalski, "Cell-averaging CFAR for multiple target situations," *IEE Proc.,* vol.133, Pt.F, no.2, 1986, pp.176-186.

[8] M. Barkat S. D. Himonas and P. K. Varshney, "CFAR detection for multiple target situations," *IEE Proc.*, vol.136, Pt.F, no.5, 1989, pp.193-209.

Chang-Joo Kim was born in Kongju on December 21, 1956. He received the B.S. degree in electronics engineering from Hankuk Aviation University in 1980, and the M.S. and Ph. D. degrees in electrical engineering from the Korea Advanced Institute of Science and Technology (KAIST) in 1988 and 1993, respectively. From 1980 to 1982 he was engaged as a research engineer at Agency for Defence Division (ADD). Since 1983 he has been with the communication fields of ETRI, where he is now head of the Radio Signal Processing Section. His current interests include signal detection, channel coding, and digital signal processing.

Hwang-Soo Lee was born in Seoul, Korea, in 1952. He received the B. S. degree in electrical engineering from Seoul National University, Seoul, in 1975, and the M.S. and Ph. D. degrees in electrical engineering from the KAIST, Seoul in 1978 and 1983, respectively. In 1975 he was with the Hyundai Heavy Industries Co., where he was involved in designing marine instrumentation and automatic navigation systems. In March 1983, he joined KAIST as an Assistant Professor of electrical engineering. He is currently a Professor in the Department of Information and Communication Engineering at KAIST Seoul Campus. His current research interests include spoken language processing, digital data transmission, and design of mobile communication systems.